Unlocking Biradical Character in Diborepins

Kimberly K. Hollister,[a,b] Andrew Molino,[c] Nula Jones,[a] VuongVy V. Le,[a] Diane A. Dickie,[a] David S. Cafiso,[a] David J. D. Wilson,[c]* and Robert J. Gilliard, Jr.[b]*

[a]Department of Chemistry, University of Virginia, Charlottesville, Virginia 22904, United States

[b]Department of Chemistry, Massachusetts Institute of Technology, 77 Massachusetts Avenue, Building 18-596, Cambridge, MA 02139-4307, United States

[c]Department of Chemistry and Physics, La Trobe Institute for Molecular Science, La Trobe University, Melbourne, 3086, Victoria, Australia

ABSTRACT: Systems that possess open- and closed-shell behavior attract significant attention from researchers due to their inherent redox and charge transport properties. Herein, we report the synthesis of the first diborepin biradicals, which display tunable biradical character based on the steric and electronic profile of the stabilizing ligand and the resulting geometric deviation of the diborepin core from planarity. While there are numerous all-carbon-based biradical systems, boron-based biradical compounds are comparatively rare, particularly ones in which the radical sites are disjointed. Calculations using DFT and multireference methods demonstrate that the fused diborepin scaffold exhibits high biradical character up to 95%. Use of a non-sterically demanding diaminocarbene promotes the planarization of the pentacyclic framework, resulting in the synthetic realization of a diborepin containing a dibora-quinoidal core, which possesses a closed-shell ground state and thermally accessible triplet state. The biradicals were structurally authenticated and characterized by both solution and solid-state EPR spectroscopy. Half-field transitions were observed at low temperatures (ca. 170 K), confirming the presence of the triplet state. Initial reactivity studies of the biradicals led to the isolation and structural characterization of a bis(borepin hydride) and bis(borepin dianion).

Introduction

Boron-doped polycyclic aromatic hydrocarbon (PAH) radicals have garnered significant attention from scientific communities concerned with understanding novel electronic structures and chemical bonding.[1] Due to their electronic flexibility, these molecules have also begun to spark the interest of researchers whose efforts focus on the development of new types of devices and molecular materials.[2] Specifically, radicals often give rise to unusual spin states and possess the ability to undergo oxidative and reductive transformations, an important criterion for systems that rely on redox processes and charge transport.[3] While boron-centered monoradicals have been studied in detail, diradicals are rare but engender an element of bifunctionality (i.e., *inter*- or *intra*-molecular reactions and phenomena at more than one site).[4] These diradicals often adopt the preferred closed-shell electronic structure due to the inherent propensity of electrons to couple.[4-5] However, with appropriate molecular design approaches, open-shell molecules can be realized in which there are two unpaired spins with minimal interaction on a single molecule. These species are commonly referred to as biradicals, where the percentage of unpaired spins can be measured and characterized by their biradical character (y = 0 represents a closed-shell structure and y = 1 is purely open-shell).[6] Frequently, the terms 'diradical' and 'biradical' are used synonymously. However, in this study, such species are distinguished based on the magnitude of the magnetic exchange interaction (J). In diradicals, the unpaired electrons are in close spatial

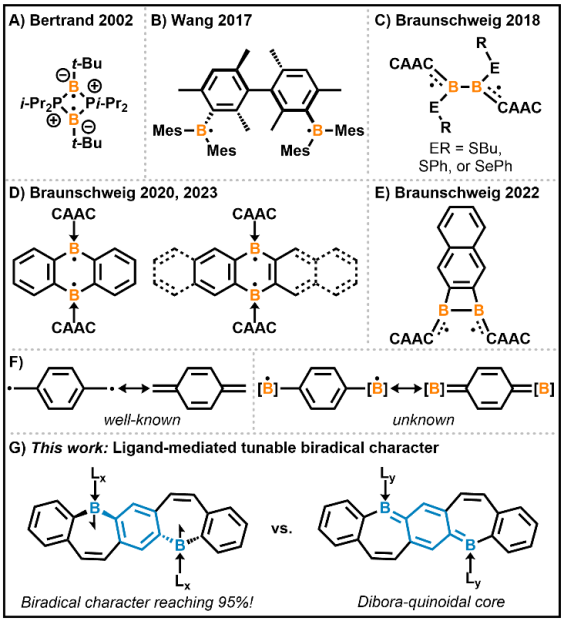

Figure 1. A) B_2P_2-cyclobutane diradical; B) Bis(mesitylene)-linked diboron biradical; C) CAAC-stabilized diradical congener of diborane; D) CAAC-stabilized diboraanthracene, diboranaphthalene, and diborapentacene biradicals; E) 1,2-diborete biradicaloid; F) p-quinodimethane framework with open- and closed-shell structures (left) and boron-doped framework with open-shell structure and closed-shell dibora-quinone (right); G) *This work*: Borepin biradicals with open-shell singlet ground state and Dibora-quinone.

Scheme 1. Synthesis of fused bis(haloborepin) **2** and Lewis-base stabilized adducts **3**-**6**.

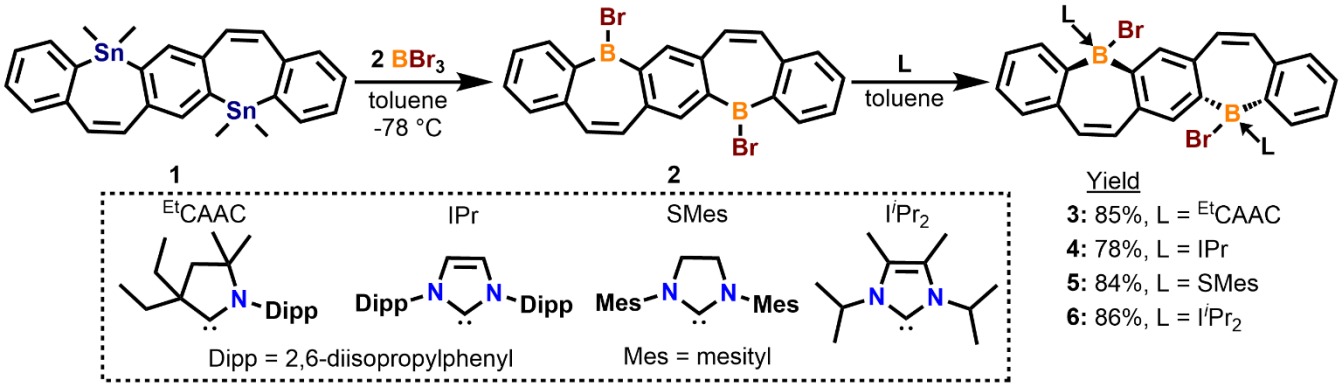

proximity, leading to a strong magnetic exchange interaction, whereas in biradicals, the spatial separation or electronic configuration results in a weak or nearly negligible exchange interaction.[6a] For carbon-based organic compounds, biradicals are significantly more common and have already found applications in molecular electronics and switches, singlet fission, non-linear optics, as well as for the activation of energy-relevant small molecules.[4-5, 7] Seminal work by Bertrand detailed the isolation of a B_2P_2 cyclobutane-type singlet diradical species and its linked tetraradical (Figure 1A).[8] As the boron atoms are in close proximity within the same ring, there is through-space coupling between the two radical sites. Wang and coworkers isolated a diboron biradical linked with a bis(mesitylene) backbone that displayed a triplet ground state (Figure 1B).[9] Shortly thereafter, Braunschweig reported cyclic(alkyl)(amino) carbene (CAAC) stabilized diradicals that resulted from rotation around the boron-boron bond, leading to open-shell character (Figure 1C).[10] Harman isolated fully aromatized diboraanthracenes using the classic diamino N-heterocyclic carbenes (NHC);[11] however, Braunschweig determined that when CAACs are employed in the synthesis of reduced diboraanthracenes, open-shell compounds are obtained with high biradical character (85%),[12] which can also be extended to diboranapthalene and diborapentacene (Figure 1D).[13] Braunschweig also disclosed 1,2-diborete biradicaloids with 62% biradical character (Figure 1E).[14] Despite these valuable contributions to the field, there are no examples of boron biradicals where the boron atoms are positioned in separate rings of PAHs; therefore, the impact of spatial separation on biradical tuning is not well understood. Moreover, the commonly observed conversion between carbon-based p-quinodimethane closed- and open-shell states remains hitherto unknown for diboron systems (Figure 1F).

Our laboratory has been investigating the chemistry of borepins, where the parent 7-membered boracycle is aromatic with 6π electrons.[15] These molecules date back to the early work of van Tamelen, Brieger, and Untch six decades ago.[16] Since then, there have been a number of key contributions to the field in terms of developing synthetic routes to new borepins as well as understanding their optical and electronic properties.[17] While a significant number of even-electron neutral borepins have been characterized and discussed in the chemical literature,[17] odd-electron and ionic borepins were only recently disclosed by our laboratory.[18] Consequently, the chemical reactivity of reduced borepins remains unestablished, which contrast with the known chemistry of smaller 5- and 6-membered reduced boron-doped PAHs, which have experienced rapid development.[11-13, 19] Herein, we report the first series of borepin biradicals (**7**–**10**). Notably, compounds **7**–**9** feature two disjointed radical sites on a pentacyclic scaffold with biradical character up to 95% — among the highest observed thus far for boron diradicals. Moreover, modulation of the steric parameters of the stabilizing ligands controls the geometric bending of the diborepin framework, thus unveiling a biradical tuning strategy. When the diborepin core is planarized, an unprecedented dibora-quinoidal core has been observed in compound **10** (Figure 1G). Initial reactivity studies of the borepin biradicals led to the isolation of bis(borepin hydride) **12** and bis(borepin anion) **14**.

Results and Discussion

A double tin-boron exchange between Tovar's fused bis-stannacycle (**1**)[17b] and BBr_3 resulted in the highly air- and moisture-sensitive fused bis(bromo-dibenzo[*b,f*]borepin) (**2**), isolated as a red solid in 73% yield (Scheme 1). The $^{11}B\{^1H\}$ NMR spectrum showed the presence of one signal at 62.6 ppm, consistent with tricoordinate boron-halogen bonded species.[20] It should be noted that the chloride analogue of **2** has been previously generated in-situ but never isolated or characterized,[17b] and **2** is one of very few examples of isolated tricoordinate halo-borepins.[21] The tetracoordinate, Lewis-base stabilized adducts **3**-**6** with EtCAAC [2,6-diisopropylphenyl)-4,4-diethyl-2,2-dimethyl-pyrrolidin-5-ylidene],[22]IPr [1,3-bis(2,6-diisopropylphenyl)imidazol-2-ylidene],[23] SMes [1,3-bis(2,4,6-trimethylphenyl)imidazolidin-2-ylidene],[23] and I^iPr_2 [1,3-diisopropyl-4,5-dimethylimidazol-2-ylidene][24] ligands were isolated in 78–86% yields by stirring a toluene solution of **2** with the corresponding carbene at room temperature. Characterization by NMR proved to be challenging due to the low solubility of the compounds, slow rotation of the ligands, and asymmetry across the fused borepin (FBP) core. At room temperature, ligand-centered protons were broad and indistinguishable but resolved as the samples were heated (see supporting information for details). Bright red needle-like single crystals of **2** suitable for X-ray diffraction were grown by slow-cooling a hot chlorobenzene solution. The solution was heated to 130 °C, demonstrating impressive thermal stability for a Lewis-acidic boracycle. The FBP core is planar, and displaced π-stacking is observed with interactions between the boron atoms and adjacent 7-membered borepin ring (Figure 2A, B–centroid distance 3.636 Å) and the C=C bond on the borepin backbone and adjacent 7-membered ring (Figure 2A, C=C–centroid distance 3.464 Å). Crystals of compounds **3**-**6** were grown from concentrated

Scheme 2. Synthesis of compounds **7**-**10.**

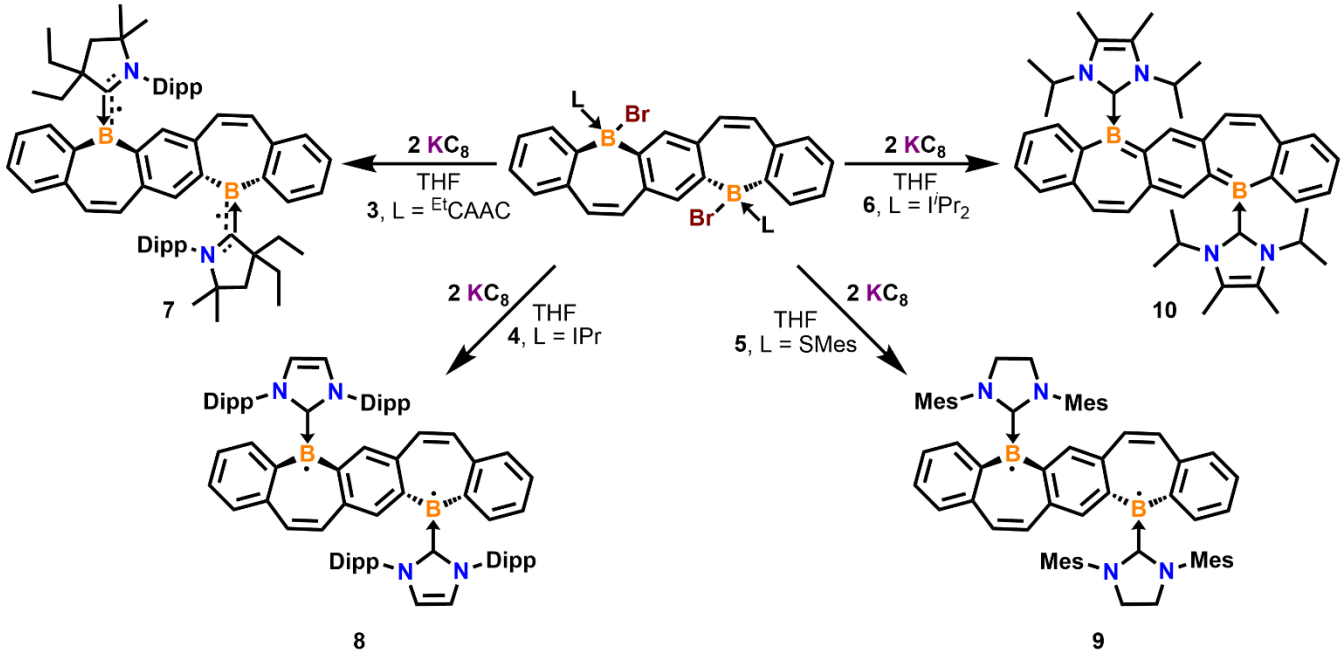

The dashed line in compound **7** indicates that the majority of the unpaired spin density resides on the N, C, B fragment. Meanwhile, in compounds **8** and **9**, the most significant portion of the spin density is boron localized, with additional contributions on the carbene carbon atoms. Compound **10** is drawn based on its structural information and the closed-shell ground state predicted by DFT (*vide infra*).

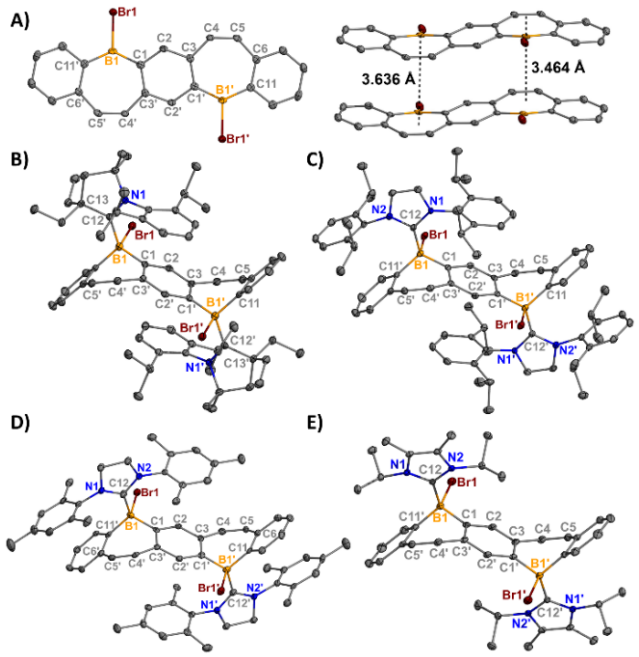

Figure 2. Molecular structures of **2** (A, displaced π-stacking shown in right image), **3** (B), **4** (C), **5** (D) and **6** (E). (Thermal ellipsoids at 50% probability; H atoms and co-crystallized solvent were omitted for clarity; for **5**: only one of two crystallographically independent molecules shown). Selected bond lengths [Å] and angles [°]: **2**: B1–Br1 1.962(3), B1–C1 1.551(4); **3**: B1–Br1 2.1457(18), B1–C1 1.613(3), B1–C12 1.675(3); **4**: B1–Br1 2.133(2), B1–C1 1.621(3), B1–C12 1.652(3); **5**: B1–Br1 2.120(5), B1–C1 1.636(6), B1–C12 1.664(7); **6**: B1–Br1 2.1158(13), B1–C1 1.6195(17), B1–C12 1.6430(17).

solutions of THF and characterized by single-crystal X-ray diffraction (Figure 2B-E). The B1–Br1 bond lengths [2.1158(13)-2.1457(18) Å] are elongated compared to the halo-borepin [**2**, 1.962(3) Å], which is consistent with increased electron density at the boron center. The B1–C1 [1.613(3)-1.634(7) Å] and B1–C12 [1.6430(17)-1.679(7) Å] bond distances in **3**-**6** are consistent with boron-carbon single bonds.[20] The FBP core is significantly distorted from planarity in the tetracoordinate adducts, and angles were measured with planes drawn through the boron center and adjacent six-membered rings (Figure S36). The distortion from planarity increased from compound **5** [55°] to **4** [59°] to **6** [62°] to **3** [68°]. π-interactions were observed in **4** between the inner diisopropylphenyl (Dipp) groups and central FBP ring [3.6457(15) Å] and the outer Dipp groups and terminal FBP rings [3.7184(16) Å]. This was also observed in **5** between the outer mesityl groups and terminal FBP rings [3.536(3) Å].

Compounds **3**-**6** were then subjected to two-electron reductions with the addition of a slight excess of potassium graphite (KC_8) to afford NMR-silent compounds **7**–**10** (Scheme 2). Compound **7** was isolated as a yellow-brown solid in 66% yield, **8** and **9** as dark reddish-brown solids in 81% and 68% yields, respectively, while compound **10** was isolated as a dark blue solid in 61% yield. Compound **7** crystallized as yellow plates from concentrated THF at -37 °C (Figure 3A), **8** as orange blocks from concentrated hexanes at -37 °C (Figure 3B), **9** as yellow plates from concentrated toluene at -37 °C (Figure 3C), and **10** as dark blue blocks from the slow evaporation of toluene at room temperature (Figure 3D). In the FBP core, compounds **7**-**9** exhibited varying levels of distortion from planarity, with all compounds possessing approximate C_i symmetry. In contrast, the FBP core in compound **10** was observed to be planar, with the planes of the coordinating ligands positioned perpendicular to the FBP core, representing approximately C_{2h} symmetry. The distortion of the fused core results from π- and/or steric interactions between the corresponding carbene ligands and aromatic rings of the FBP. Both compounds **8** and **9**

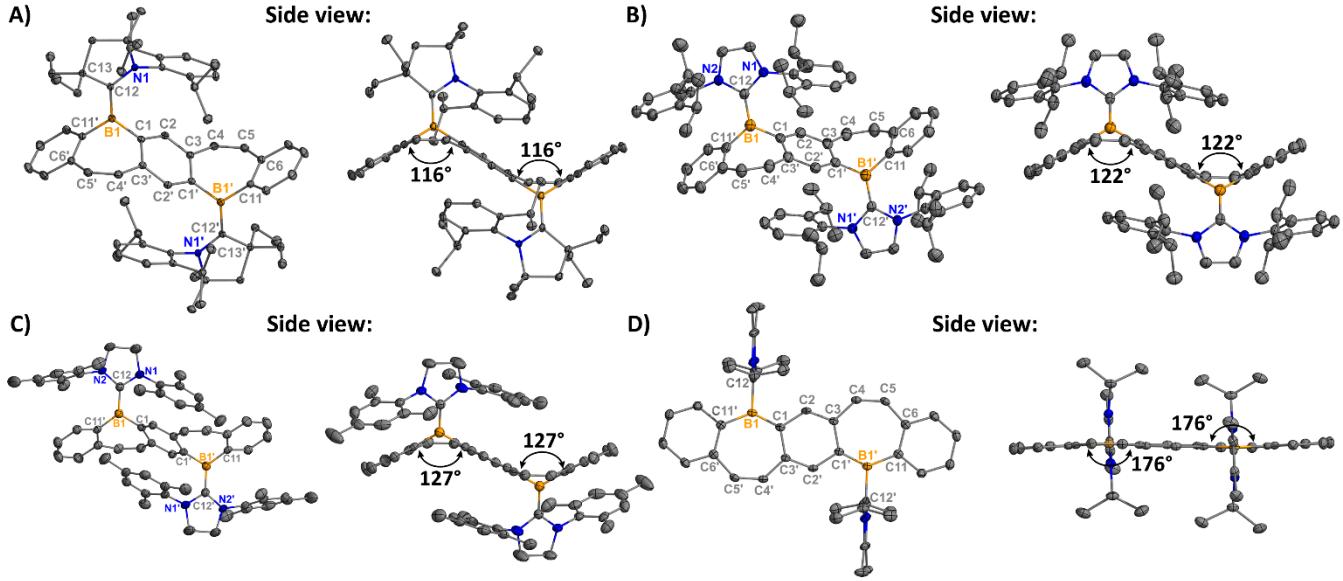

Figure 3. Molecular structures of **7** (A), **8** (B), **9** (C) and **10** (D) with side views (right of structure). (Thermal ellipsoids at 50% probability; H atoms were omitted for clarity. Angles were measured by drawing planes through the boron center and adjacent six-membered rings. Selected bond lengths [Å] and angles [°]: **7**: B1–C1 1.5773(16), B1–C12 1.5302(16), C12–N1 1.3794(13), N1–C12–B1–C1 -17.86(18); **8**: B1–C1 1.563(4), B1–C12 1.529(4), C12–N1 1.396(3), N1–C12–B1–C1 3.0(4); **9**: B1–C1 1.572(3), B1–C12 1.525(3), C12–N1 1.395(3), N1–C12–B1–C1 12.8(4); **10**: B1–C1 1.4838(17), B1–C12 1.6058(16), C12–N1 1.3483(15), N1–C12–B1–C1-89.15(14).

display geometries consistent with non-covalent π-interactions between the Dipp (IPr) and mesityl (SMes) groups of the ligand and the FBP inner and outer rings. Considering these factors, we evaluated the degree of deviation from planarity within the FBP core, which showed a sequential reduction in the planar distortion in the order: **7** (64°) > **8** (58°) > **9** (53°) > **10** (4°). A slight decrease in the $^{(carbene)}$C12–B1 bond was observed in compounds **7**–**9** compared to their tetracoordinate adducts, but **10** retained its C12–B1 single bond character. A decreased bond length between B1–C1 [1.4838(17) Å] was observed in **10** compared to **7**–**9** [1.563(4)-1.5773(16) Å], indicating double bond character. Collectively, these geometrical data suggest that steric factors may be used to alter the electronic structure of reduced diborepins, and the core structure of compound **10** may be viewed as a dibora-quione.

EPR analyses of compounds **7**–**10** were conducted in dilute toluene solutions (Figures 5A S24, S29). Initially, at room temperature, the characteristic half-field transition of $\Delta m_s = \pm 2$ was not detected in these compounds. This observation aligns with behaviors seen in other disjointed main-group biradicals, characterized by large inter-spin distances and minimal zero-field splitting (ZFS) parameters.[25] In such cases, the half-field transition intensity inversely correlates with the sixth power of the inter-spin distance ($I(\Delta m_s = \pm 2) \propto r^{-6}$). However, with the temperature lowered and the microwave power increased, the half-field transition became detectable in compounds **7**–**9**, confirming the presence of a biradical species. Compounds **7**-**9** also exhibited a relatively intense transition, centered between the ZFS transitions of the triplet-state, which is proposed to originate from a superimposed monoradical impurity. The detection of a monoradical impurity is consistent with recent reports of carbene-stabilized boron biradicals,[12, 14, 18c, 27] where even the smallest amount of monoradical is detectable by EPR.

Simulated EPR parameters for compounds **7**–**9** revealed distinctive electronic characteristics, primarily reflected in the axial ZFS parameter, *D*. Compounds **7**–**9** exhibit isotropic g-values of approximately 2.012; however, there is notable variation in their ZFS parameters (see ESI for comparison of axial and rhombic models). The *D* values of **7**–**9** span from 0.0070 to 0.0097 cm^{-1} (Figure 5A and Tables S4–6). Notably, **8** and **9**, coordinated to diamino carbenes (IPr and SMes), exhibit *D* values of 0.00911 cm^{-1} and 0.00972 cm^{-1} respectively. These values are appreciably higher than the *D* value of 0.0070 cm^{-1} found in **7**, which is coordinated with ^{Et}CAAC. The relatively low *D* values observed for compounds **7**–**9** imply a considerable spin-spin separation, suggesting weaker dipolar interactions. This observation contrasts recent reports of open-shell carbene-stabilized diboracycles, where boron centers, whether directly bonded (r = 1.701 Å), or in close spatial proximity (r = 2.748 Å), exhibit substantially larger *D* values in the range of 0.0284–0.0319 cm^{-1}.[12, 14] The simulated *D* values for compounds **7**–**9** were utilized in conjunction with the point-dipole approximation to estimate their average spin-spin distances.[26] This approach yielded an average distance range of 6.59–7.19 Å, which shows a notable correlation with the distances between the centroids of the two N-$^{(carbene)}$C-B moieties measured from the single crystal X-ray structures of these compounds, ranging from 6.88 to 7.50 Å (Table S7). Theoretically computed spin-density distribution plots for the triplet electronic states of compounds **7**–**9** substantiate their dipolar characteristics. These plots distinctly show two regions of α spin density, each localized to a B-$^{(carbene)}$C-N moiety (Figure 4). In contrast, planar FBP **10** exhibits a distinctly different distribution pattern, with α spin density delocalized over the entire FBP core, indicative of co-extensive spin characteristics (*vide infra*).

Variable-temperature EPR studies demonstrated a temperature-dependent signal intensity in the $\Delta m_s = \pm 1$ region (Figure 5B, S25, S29). As the temperature decreased, the

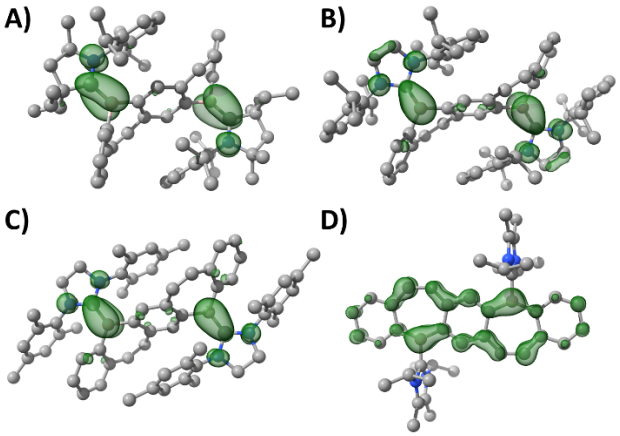

Figure 4. Spin density distribution plots for the triplet configuration of **7** (A), **8** (B), **9** (C), and **10** (D). (Isosurface = ±0.003 $e\,a_0^3$).

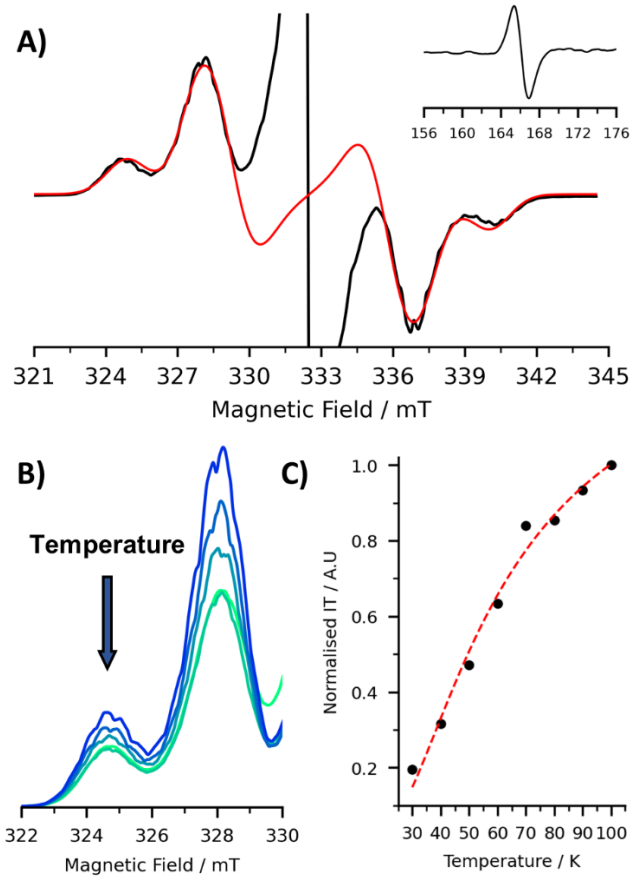

Figure 5. A) Experimental CW X-band (9.81 GHz) (black trace) and simulated (red trace) EPR spectra of **7** in a toluene solution at 80 K with the half-field transition shown in the inset. (Experimental parameters: 250 G scan of the allowed transitions at 2 G modulation amplitude and 2.005 mW of power. 100 G scan of the half field transition at 8 G modulation amplitude and 20.04 mW of power. Solutions were prepared at a concentration of less than 2 mM.) (Simulation parameters: g_{iso} = 2.012, D/hc = 0.0070 cm^{-1}, E/hc = 0.0005 cm^{-1}, RMSD = 0.0076). B) Expanded view of the Δm_s = ±1 transitions in the VT-EPR spectra of **7** over a temperature range of 100–20 K. C) *IT*–*T* plot of the Δm_s = ±2 transition of **7** in toluene from 30–100 K with the Bleaney-Bowers fit in red (ΔE_{ST} (-*J*) = -0.452 kJ mol^{-1}, R^2 = 0.992).

signal intensity for compounds **7**–**9** diminished, suggesting these compounds have an open-shell singlet ground state. Conversely, compound **10** displayed a weak EPR signal at room temperature in toluene, which vanished upon cooling to 170 K (Figure S33) and reemerged upon warming. Such behavior suggests a closed-shell ground state for **10**, with a thermally accessible triplet state. For compounds **7**–**9**, the singlet-triplet gaps (ΔE_{ST}) were experimentally determined by fitting the product of the integrated signal intensity and temperature (*IT*) with respect to temperature using the Bleaney-Bowers equation (Figures 5C, Table S3).[28] The singlet-triplet gap ($\hat{H} = -JS_AS_B$) was found to correlate with the degree of distortion from planarity within the FBP moiety: **7** (64°; -0.45 kJ mol^{-1}) < **8** (58°; -0.57 kJ mol^{-1}) < **9** (53°; -0.75 kJ mol^{-1}). This observed trend implies that increased ligand sterics lead to a smaller singlet-triplet gap, thereby enhancing the biradical character.

Theoretical calculations were performed to determine the electronic structure and spin preferences of compounds **7**–**10**. Relative adiabatic energies, calculated at the B3LYP-D3(BJ)/def2-TZVP(-f) level of theory, reveal that compound **7**–**9** possess open-shell singlet (OSS) ground states with a low-lying triplet (T) state ($\Delta E_{OSS\text{-}T}$ = -0.2 to -1.1 kJ mol^{-1}, Table 1). Conversely, compound **10** was found to possess a closed-shell singlet (CSS) ground state with a calculated singlet-triplet gap ($\Delta E_{CSS\text{-}T}$) of -35.3 kJ mol^{-1}. Examination of the broken-symmetry (BS) wavefunction for **7**–**9** reveals moderate anti-ferromagnetic exchange coupling (J = -17 to -105 cm^{-1}), qualitatively reproducing those obtained experimentally.[29] Additionally, it was determined that the paramagnetic centers are localized within the two N-$^{(carbene)}$C-B moieties. The OSS spin-density plots for compounds **7**–**9** clearly illustrate the separation between the two spin-sites. This observation is further validated by the calculated natural atomic spin populations, which indicate that between 85–92% of the spin density is localized to the two N-$^{(carbene)}$C-B moieties (N: ±0.15, $^{(carbene)}$C: ± 0.24, B: ±0.38) (Figure 6A and Table S10). Moreover, the orbital overlap ($|S^{\alpha\beta}|$), for the magnetically coupled orbitals of compounds **7**–**9** was calculated to be close to zero (0.043–0.121). This suggests that these orbitals are non-coextensive, a characteristic of disjointed biradical species with pronounced biradical character.[30] To obtain a more accurate determination of $\Delta E_{OSS\text{-}T}$ and quantify the biradical nature of compounds **7**–**9**,

Table 1. Calculated relative electronic energies (kJ mol^{-1}), exchange coupling (cm^{-1}), magnetic orbital overlaps, biradical index, and experimentally determined singlet-triplet gaps (kJ mol^{-1}) of **7**–**9**.

BS-DFT	**7**	**8**	**9**
$\Delta E_{CSS\text{-}T}$[a]	+80.08	+50.21	+47.01
$\Delta E_{OSS\text{-}T}$	-0.197	-0.599	-1.145
J	-17	-53	-105
$\|S^{\alpha\beta}\|$	0.043	0.086	0.121
DLPNO-NEVPT2			
$\Delta E_{OSS\text{-}T}$	-0.403	-0.522	-1.082
HONO Occ.	1.025	1.044	1.056
LUNO Occ.	0.975	0.956	0.944
γ	0.950	0.912	0.888
Bleaney-Bowers Fit			
$\Delta E_{ST} = J$	-0.451 ± 0.020	-0.570 ± 0.054	-0.745 ± -0.050

[a] B3LYP-D3(BJ)/def2-TZVP(-f) (CPCM, THF)

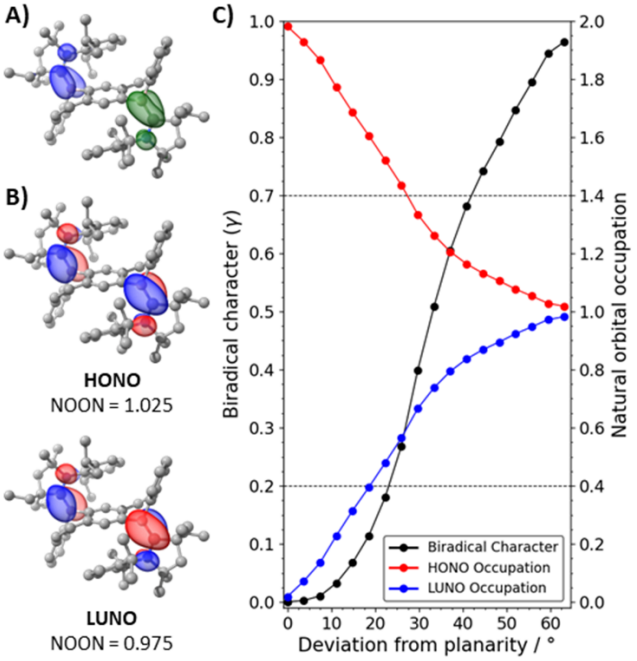

Figure 6. A) Open-shell singlet spin-density distribution of **7** (Isosurface = ±0.003 *e* a_0^3, green and blue correspond to regions α- and β-spin, respectively). B) Optimized CASSCF natural orbitals and natural orbital occupation numbers (NOON) of **7** (Isosurface = ±0.025 *e* a_0^{-3}). C) Scan of *y* and NOON with respect to planar deviation for **10** at the CASSCF(2,2)/def2-TZVP level of theory.

higher-level *ab initio* calculations were performed, accounting for both static and dynamic electron correlation. Complete active space self-consistent field (CASSCF) calculations employed an active space of two electrons in two orbitals (CASSCF(2,2)/def2-TZVP) (see SI for investigations of additional active spaces). The natural orbital occupation numbers (NOON) for the optimized singlet-ground states in **7**–**9** are close to unity, confirming an open-shell singlet ground state (Table 1 and Figure 6B). Inclusion of dynamic electron correlation via the DLPNO-NEVPT2 method yields OSS-T gaps ($\Delta E_{OSS\text{-}T}$), equivalent to the exchange interaction *J*, that are consistent with those determined experimentally: **7** (-0.403 kJ mol^{-1}) < **8** (-0.522 kJ mol^{-1}) < **9** (-1.082 kJ mol^{-1}).[31] Complementary to these results, compounds **7**-**9** were also found to possess significant biradical character (*y*) following the same progression: **7** (0.950) > **8** (0.913) > **9** (0.888). These trends highlight the correlation between the deviation from planarity of the FBP core and its dynamic biradical properties. With this understanding, we sought to determine the scope of biradical tuneability. A CASSCF(2,2)/def2-TZVP scan of the ground-state singlet potential energy surface with respect to FBP plane distortion for **10** reveals that FBP species with biradical characters in the range of 0.7–1.0 may be accessed when the planar deviation is greater than 42° (Figure 6C). Moreover, planar deviation angles between 22 and 42° are expected to exhibit biradicaloid character.

To better understand the electronic differences between compounds **7**-**9**, we tested their ability to serve as radical-based synthons and employed tributyltin hydride as a H• donor for the formation of borepin hydrides **11**-**13** (Scheme 3). Consistent with its high spin localization on boron, compound **8** reacted with excess Bu_3SnH in minutes to give the bis(IPr-stabilized borepin hydride) **12** in 75% yield. Compound **12** was fully characterized and showed a characteristic tetracoordinate boron peak in the $^{11}B\{^1H\}$ spectrum at -11.82 ppm that resolved into a doublet at 80 °C in the ^1H coupled spectrum. ^1H NMR studies showed a very broad signal at 3.69 ppm that resolved into a sharp singlet when the ^{11}B decoupler was turned on, corresponding to the B–H protons. Compound **12** was structurally characterized via X-ray diffraction after colorless single crystals were grown from a toluene/hexanes mixture (Figure 7A). It should be noted that borepin hydrides have historically been considered unstable and synthetically challenging to isolate.[15-16] Compound **12** is a rare example of a structurally authenticated borepin hydride, with only one other example reported,[32] and a few others suggested based on IR[16] or NMR data.[33] Structurally, **12** is very similar to **4** and the B1–C1 [1.613(2) Å] and B1–C12 [1.635(2) Å] bonds are in line with the expected boron-carbon single bond lengths. While compound **9** has comparable spin density on boron, its biradical character is lower, and thus the reaction to form the bis(SMes-stabilized borepin hydride) **13** required additional time and still showed the presence of a paramagnetic species, which suggests an incomplete reaction. Accordingly, compound **7**, which has significantly lower spin density on boron, did not react at all at room temperature and required heating to 100 °C for the reaction to proceed to the bis(CAAC-stabilized borepin hydride) **11**. Despite challenges surrounding the isolation of **11** and **13** they could be detected using ^{11}B NMR, with peaks at -1.88 and -12.70 respectively. This trend in reactivity illustrates that radical character plays an important role in dictating chemical reactivity.

Scheme 3. Reactivity of fused diborepin biradicals.

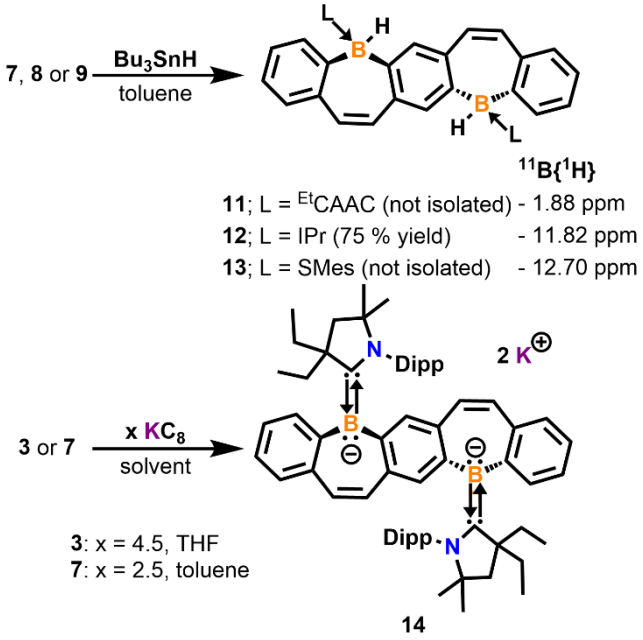

To provide further insight into reactivity trends, attempts were made to reduce each biradical to its corresponding anion. The reduction of **4** in THF led to activation of the IPr ligand and fused borepin backbone, and a few crystals from that reaction were characterized by X-ray diffraction (Figure S37). Using compounds **8**–**10** as a starting point for reduction, there was no evidence for the formation of

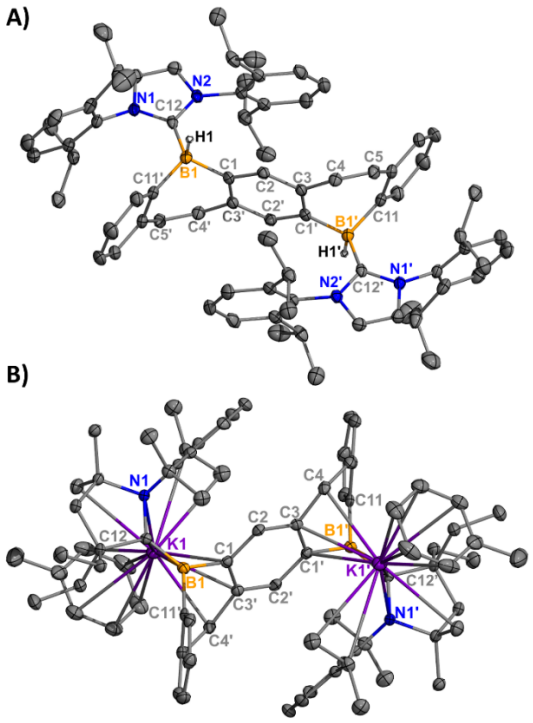

Figure 7. Molecular structures of **12** (A) and **14** (B). (Thermal ellipsoids at 50% probability; H atoms were omitted for clarity except for the B–H atoms in **12**. Selected bond lengths [Å] and angles [°]: **12**: B1–C1 1.613(2), B1–C12 1.635(2), C12–N1 1.3663(17); **14**: B1–C1 1.595(2), B1–C12 1.468(2), B1–K1 3.039(2), C12–N1 1.480(2), N1–C12–B1–C1 -5.8(3).

NHC-stabilized bis(borepin anions). Reactions resulted in rapid decomposition to the corresponding hydridoboron compound (for **8** and **9**) or unidentified tetracoordinate boron species (for **10**), observed via NMR. Distinct from the results observed for **8**–**10**, compounds **3** and **7** were used to successfully synthesize bis(^{Et}CAAC-stabilized borepin anion) **14** as highly air- and moisture-sensitive dark red solids in 81 and 52% isolated yields, respectively. Yellow, plate-like single crystals of **14** were grown from a concentrated solution of toluene at -37 °C (Figure 7B). The potassium atoms are encapsulated between the N-Dipp group of the ^{Et}CAAC ligand, a molecule of toluene, and one half of each borepin ring. The C12–B1($^{(carbene)}$C–B) bond (1.468(2) Å) is significantly shortened compared to its biradical counterpart **7** [1.5306(16) Å], and the torsion angle N1–C12–B1–C1 [5.9(3)°] is small, resulting in double bond formation. Consistent with the high reactivity of the compound, NMR analysis proved challenging, again rapidly decomposing to the corresponding hydridoboron compound. In order to obtain NMR data, a piece of freshly cut potassium metal was placed inside the NMR tube during data collection. An ^{11}B{^{1}H} NMR resonance was observed at 21.7 ppm, which is consistent with reported compounds containing tricoordinate negatively charged, electron-rich boron centers.[18c] It should be noted that this method of adding excess reducing agents (i.e., KC_8, Na/NaCl, and cobaltocene) to the NMR tube was used with **8**-**10**, but the corresponding anion was never observed spectroscopically, and the compounds continued to degrade into unidentified boron-containing species over time. These reactivity studies are consistent with the electronic structures of the biradical starting materials. The non-isolable NHC-stabilized diborepin dianions would have electronic structures where the added electron must populate the boron p-orbital and/or those in the borepin ring (i.e., the ^{carbene}C p-orbital is largely filled by the adjacent N lone pairs). This results in highly electron-rich boron heterocycles that are extremely reactive. In contrast, the isolable CAAC-stabilized diborepin dianion takes advantage of the stronger π-accepting nature of CAAC, where additional electron density may reside on the ligand, thereby mitigating the reactivity of the dianion.

Conclusion

In conclusion, we have isolated the first examples of borepin biradicals, which contain stable disjointed boron radical sites with high biradical character (up to 95%). Structural analysis, along with computational support, indicates that the biradical character can be tuned by modulating both the sterics and electronics of the supporting carbene ligand, allowing for the isolation of a borepin compound containing a dibora-quinoidal core. It is noteworthy that the comparable carbon-based fragment, p-quinodimethane, has attracted the interest of researchers across chemistry disciplines due to its unique electronic structure and ability to fluctuate between the open-shell diradical and closed-shell quinone states.[34] The potential in electronic and optical materials, along with their increased reactivity, has led researchers to modify such scaffolds and incorporate them into various PAHs.[34] To our knowledge, there are no examples in which boron atoms are incorporated into the two para positions. This type of tunable radical character, with the choice of a sterically appropriate coordinating ligand or selective functionalization of the FBP core, may result in a diverse range of FBPs with distinct biradical properties and applications. Initial reactivity studies indicate that these molecules behave as true boron biradicals, leading to bis(borepin hydride)s and a bis(borepin anion). Additional investigations into the reactivity of these reduced diborepins, as well as related structures, are currently underway in our laboratory.

ASSOCIATED CONTENT

Supporting Information. The supporting information file contains experimental details, NMR spectra, EPR spectra, UV/vis spectra, single-crystal X-ray diffraction data, and computational details (PDF). This material is available free of charge via the Internet at http://pubs.acs.org." CCDC 22166425–2266436 contain the supplementary crystallographic data for this paper. These data can be obtained free of charge from the Cambridge Crystallographic Data Center via www.ccdc.cam.ac.uk/structures .

AUTHOR INFORMATION

Corresponding Author

* **David J. D. Wilson** - Department of Chemistry and Physics, La Trobe Institute for Molecular Science, La Trobe University, Melbourne, 3086, Victoria (Australia); orcid.org/0000-0002-0007-4486; Email: David.Wilson@latrobe.edu.au

* **Robert J. Gilliard, Jr.** - Department of Chemistry, Massachusetts Institute of Technology, Cambridge, Massachusetts 02139-4307, United States; orcid.org/0000-0002-8830-1064; Email: gilliard@mit.edu

Author Contributions

Kimberly K. Hollister - Department of Chemistry, Massachusetts Institute of Technology, Cambridge, Massachusetts 02139-4307, United States; orcid.org/0000-0001-9024-4436
Andrew Molino - Department of Chemistry and Physics, La Trobe Institute for Molecular Science, La Trobe University, Melbourne, 3086, Victoria (Australia); orcid.org/0000-0002-0954-9054
Nula Jones - Department of Chemistry, University of Virginia, Charlottesville, Virginia 22904, United States; https://orcid.org/0009-0003-4329-7457
VuongVy V. Le - Department of Chemistry, University of Virginia, Charlottesville, Virginia 22904, United States; orcid.org/0009-0003-6665-1180
Diane A. Dickie - Department of Chemistry, University of Virginia, Charlottesville, Virginia 22904, United States; orcid.org/0000-0003-0939-3309
David S. Cafiso - Department of Chemistry, University of Virginia, Charlottesville, Virginia 22904, United States; orcid.org/0000-0002-3813-8721

The manuscript was written through contributions of all authors. / All authors have given approval to the final version of the manuscript.

Notes

The authors declare no competing financial interest.

ACKNOWLEDGMENT

We are grateful to the University of Virginia (UVA), Massachusetts Institute of Technology (MIT), and the National Science Foundation Chemical Synthesis (CHE 2046544) and Major Research Instrumentation (CHE 2018870) programs for support of this work. RJG acknowledges additional laboratory support through a Beckman Young Investigator award from the Arnold & Mabel Beckman Foundation. K.H acknowledges the AAUW for an American Dissertation Year Fellowship to support her research. Generous allocations of computing resources from the National Computational Infrastructure (NCI), Intersect, and La Trobe University are also acknowledged.

ABBREVIATIONS

FBP, fused borepin; NHC, N-heterocyclic carbene; CAAC, cyclic(alkyl)(amino) carbene.

REFERENCES

1. (a) Su, B.; Kinjo, R., Construction of Boron-Containing Aromatic Heterocycles. *Synthesis* **2017,** *49*, 2985-3034 ; (b) Feng, Z.; Tang, S.; Su, Y.; Wang, X., Recent advances in stable main group element radicals: preparation and characterization. *Chem. Soc. Rev.* **2022,** *51*, 5930-5973 ; (c) Power, P. P., Persistent and Stable Radicals of the Heavier Main Group Elements and Related Species. *Chem. Rev.* **2003,** *103*, 789-810
2. (a) Vidal, F.; Jäkle, F., Functional Polymeric Materials Based on Main-Group Elements. *Angew. Chem. Int. Ed.* **2019,** *58*, 5846-5870 ; (b) Pop, F.; Zigon, N.; Avarvari, N., Main-Group-Based Electro- and Photoactive Chiral Materials. *Chem. Rev.* **2019,** *119*, 8435-8478 ; (c) He, X.; Baumgartner, T., Conjugated main-group polymers for optoelectronics. *RSC Adv.* **2013,** *3*, 11334-11350 ; (d) Wilcox, D. A.; Agarkar, V.; Mukherjee, S.; Boudouris, B. W., Stable Radical Materials for Energy Applications. *Annu. Rev. Chem. Biomol. Eng.* **2018,** *9*, 83-103
3. (a) Yuan, D.; Huang, D.; Rivero, S. M.; Carreras, A.; Zhang, C.; Zou, Y.; Jiao, X.; McNeill, C. R.; Zhu, X.; Di, C.-a.; Zhu, D.; Casanova, D.; Casado, J., Cholesteric Aggregation at the Quinoidal-to-Diradical Border Enabled Stable n-Doped Conductor. *Chem* **2019,** *5*, 964-976 ; (b) Nakano, M., Electronic Structure of Open-Shell Singlet Molecules: Diradical Character Viewpoint. *Top. Curr. Chem.* **2017,** *375*, 47
4. Bresien, J.; Eickhoff, L.; Schulz, A.; Zander, E., Biradicals in main group chemistry: Synthesis, electronic structure, and application in small-molecule activation. In *Reference Module in Chemistry, Molecular Sciences and Chemical Engineering*, Elsevier: 2021, https://doi.org/10.1016/B978-0-12-823144-9.00029-7.
5. Abe, M., Diradicals. *Chem. Rev.* **2013,** *113*, 7011-7088
6. (a) Chandra Mondal, K.; Roy, S.; Roesky, H. W., Silicon based radicals, radical ions, diradicals and diradicaloids. *Chem. Soc. Rev.* **2016,** *45*, 1080-1111 ; (b) Stuyver, T.; Chen, B.; Zeng, T.; Geerlings, P.; De Proft, F.; Hoffmann, R., Do Diradicals Behave Like Radicals? *Chem. Rev.* **2019,** *119*, 11291-11351
7. (a) Chen, Z. X.; Li, Y.; Huang, F., Persistent and Stable Organic Radicals: Design, Synthesis, and Applications. *Chem* **2021,** *7*, 288-332 ; (b) Zeng, Z.; Shi, X.; Chi, C.; López Navarrete, J. T.; Casado, J.; Wu, J., Pro-aromatic and anti-aromatic π-conjugated molecules: an irresistible wish to be diradicals. *Chem. Soc. Rev.* **2015,** *44*, 6578-6596 ; (c) Zeng, W.; Wu, J., Open-Shell Graphene Fragments. *Chem* **2021,** *7*, 358-386 ; (d) Sun, Z.; Ye, Q.; Chi, C.; Wu, J., Low band gap polycyclic hydrocarbons: from closed-shell near infrared dyes and semiconductors to open-shell radicals. *Chem. Soc. Rev.* **2012,** *41*, 7857-7889 ; (e) Hinz, A.; Bresien, J.; Breher, F.; Schulz, A., Heteroatom-Based Diradical(oid)s. *Chem. Rev.* **2023,** 10.1021/acs.chemrev.3c00255, ; (f) Dressler, J. J.; Haley, M. M., Learning how to fine-tune diradical properties by structure refinement. *J. Phys. Org. Chem.* **2020,** *33*, e4114 ; (g) Y. Gopalakrishna, T.; Zeng, W.; Lu, X.; Wu, J., From open-shell singlet diradicaloids to polyradicaloids. *Chem. Comm.* **2018,** *54*, 2186-2199
8. (a) Scheschkewitz, D.; Amii, H.; Gornitzka, H.; Schoeller, W. W.; Bourissou, D.; Bertrand, G., Singlet Diradicals: from Transition States to Crystalline Compounds. *Science* **2002,** *295*, 1880-1881 ; (b) Rodriguez, A.; Tham, F. S.; Schoeller, W. W.; Bertrand, G., Catenation of Two Singlet Diradicals: Synthesis of a Stable Tetraradical (Tetraradicaloid). *Angew. Chem. Int. Ed.* **2004,** *43*, 4876-4880
9. Wang, L.; Fang, Y.; Mao, H.; Qu, Y.; Zuo, J.; Zhang, Z.; Tan, G.; Wang, X., An Isolable Diboron-Centered Diradical with a Triplet Ground State. *Chem. Eur. J.* **2017,** *23*, 6930-6936
10. Böhnke, J.; Dellermann, T.; Celik, M. A.; Krummenacher, I.; Dewhurst, R. D.; Demeshko, S.; Ewing, W. C.; Hammond, K.; Heß, M.; Bill, E.; Welz, E.; Röhr, M. I. S.; Mitrić, R.; Engels, B.; Meyer, F.; Braunschweig, H., Isolation of diborenes and their 90°-twisted diradical congeners. *Nat. Commun.* **2018,** *9*, 1197
11. Taylor, J. W.; McSkimming, A.; Guzman, C. F.; Harman, W. H., N-Heterocyclic Carbene-Stabilized Boranthrene as a Metal-Free Platform for the Activation of Small Molecules. *J. Am. Chem. Soc.* **2017,** *139*, 11032-11035
12. Saalfrank, C.; Fantuzzi, F.; Kupfer, T.; Ritschel, B.; Hammond, K.; Krummenacher, I.; Bertermann, R.; Wirthensohn, R.; Finze, M.; Schmid, P.; Engel, V.; Engels, B.; Braunschweig, H., cAAC-Stabilized 9,10-diboraanthracenes—Acenes with Open-Shell Singlet Biradical Ground States. *Angew. Chem. Int. Ed.* **2020,** *59*, 19338-19343
13. Dietz, M.; Arrowsmith, M.; Drepper, K.; Gärtner, A.; Krummenacher, I.; Bertermann, R.; Finze, M.; Braunschweig, H., Structure and Electronics of a Series of CAAC-Stabilized Diboron-Doped Acenes from 1,4-Diboranaphthalene to 6,13-Diborapentacene. *J. Am. Chem. Soc.* **2023,** *145*, 15001-15015
14. Gärtner, A.; Meier, L.; Arrowsmith, M.; Dietz, M.; Krummenacher, I.; Bertermann, R.; Fantuzzi, F.; Braunschweig,

H., Highly Strained Arene-Fused 1,2-Diborete Biradicaloid. *J. Am. Chem. Soc.* **2022,** *144*, 21363-21370
15. Messersmith, R. E.; Tovar, J. D., Assessment of the aromaticity of borepin rings by spectroscopic, crystallographic and computational methods: a historical overview. *J. Phys. Org. Chem.* **2015,** *28*, 378-387
16. van Tamelen, E. E.; Brieger, G.; Untch, K. G., Synthesis of a borepin. *Tetrahedron Lett.* **1960,** *1*, 14-15
17. (a) Wang, L.; Ma, J.; Si, E.; Duan, Z., Recent Advances in Luminescent Annulated Borepins, Silepins, and Phosphepins. *Synthesis* **2020,** *53*, 623-635 ; (b) Caruso Jr., A.; Siegler, M. A.; Tovar, J. D., Synthesis of Functionalizable Boron-Containing π-Electron Materials that Incorporate Formally Aromatic Fused Borepin Rings. *Angew. Chem. Int. Ed.* **2010,** *49*, 4213-4217 ; (c) Mercier, L. G.; Piers, W. E.; Parvez, M., Benzo- and Naphthoborepins: Blue-Emitting Boron Analogues of Higher Acenes. *Angew. Chem. Int. Ed.* **2009,** *48*, 6108-6111 ; (d) Levine, D. R.; Caruso, A.; Siegler, M. A.; Tovar, J. D., Meta-B-entacenes: new polycyclic aromatics incorporating two fused borepin rings. *Chem. Comm.* **2012,** *48*, 6256-6258 ; (e) Messersmith, R. E.; Siegler, M. A.; Tovar, J. D., Aromaticity Competition in Differentially Fused Borepin-Containing Polycyclic Aromatics. *J. Org. Chem.* **2016,** *81*, 5595-5605 ; (f) Messersmith, R. E.; Yadav, S.; Siegler, M. A.; Ottosson, H.; Tovar, J. D., Benzo[b]thiophene Fusion Enhances Local Borepin Aromaticity in Polycyclic Heteroaromatic Compounds. *J. Org. Chem.* **2017,** *82*, 13440-13448 ; (g) Caruso, A., Jr.; Tovar, J. D., Functionalized dibenzoborepins as components of small molecule and polymeric pi-conjugated electronic materials. *J. Org. Chem.* **2011,** *76*, 2227-39 ; (h) Caruso, A.; Tovar, J. D., Conjugated "B-Entacenes": Polycyclic Aromatics Containing Two Borepin Rings. *Org. Lett.* **2011,** *13*, 3106-3109 ; (i) Adachi, Y.; Arai, F.; Sakabe, M.; Ohshita, J., Effect of the conjugation pathway on the electronic structures of p–π* conjugated polymers with fused borepin units. *Polym. Chem.* **2021,** *12*, 3471-3477
18. (a) Yang, W.; Krantz, K. E.; Freeman, L. A.; Dickie, D. A.; Molino, A.; Kaur, A.; Wilson, D. J. D.; Gilliard, R. J., Jr., Stable Borepinium and Borafluorenium Heterocycles: A Reversible Thermochromic "Switch" Based on Boron-Oxygen Interactions. *Chem. Eur. J.* **2019,** *25*, 12512-12516 ; (b) Adachi, Y.; Arai, F.; Jäkle, F., Extended conjugated borenium dimers via late stage functionalization of air-stable borepinium ions. *Chem. Comm.* **2020,** *56*, 5119-5122 ; (c) Hollister, K. K.; Yang, W.; Mondol, R.; Wentz, K. E.; Molino, A.; Kaur, A.; Dickie, D. A.; Frenking, G.; Pan, S.; Wilson, D. J. D.; Gilliard Jr., R. J., Isolation of Stable Borepin Radicals and Anions. *Angew. Chem. Int. Ed.* **2022,** *61*, e202202516
19. (a) Su, Y.; Kinjo, R., Boron-containing radical species. *Coord. Chem. Rev.* **2017,** *352*, 346-378 ; (b) von Grotthuss, E.; Prey, S. E.; Bolte, M.; Lerner, H.-W.; Wagner, M., Selective CO2 Splitting by Doubly Reduced Aryl Boranes to Give CO and [CO3]2−. *Angew. Chem. Int. Ed.* **2018,** *57*, 16491-16495 ; (c) Bartholome, T. A.; Kaur, A.; Wilson, D. J. D.; Dutton, J. L.; Martin, C. D., The 9-Borataphenanthrene Anion. *Angew. Chem. Int. Ed.* **2020,** *59*, 11470-11476 ; (d) Gilmer, J.; Budy, H.; Kaese, T.; Bolte, M.; Lerner, H.-W.; Wagner, M., The 9H-9-Borafluorene Dianion: A Surrogate for Elusive Diarylboryl Anion Nucleophiles. *Angew. Chem. Int. Ed.* **2020,** *59*, 5621-5625 ; (e) Trageser, T.; Bolte, M.; Lerner, H.-W.; Wagner, M., B-B Bond Nucleophilicity in a Tetraaryl μ-Hydridodiborane(4) Anion. *Angew. Chem. Int. Ed.* **2020**, 10.1002/anie.202000292, Ahead of Print ; (f) Protchenko, A. V.; Vasko, P.; Fuentes, M. Á.; Hicks, J.; Vidovic, D.; Aldridge, S., Approaching a Naked Boryl Anion: Amide Metathesis as a Route to Calcium, Strontium, and Potassium Boryl Complexes. *Angew. Chem. Int. Ed.* **2021,** *60*, 2064-2068 ; (g) Wentz, K. E.; Molino, A.; Freeman, L. A.; Dickie, D. A.; Wilson, D. J. D.; Gilliard, R. J., Jr., Reactions of 9-Carbene-9-Borafluorene Monoanion and Selenium: Synthesis of Boryl-Substituted Selenides and Diselenides. *Inorg. Chem.* **2021,** *60*, 13941-13949 ; (h) Wentz, K. E.; Molino, A.; Weisflog, S. L.; Kaur, A.; Dickie, D. A.; Wilson, D. J. D.; Gilliard, R. J., Jr., Stabilization of the Elusive 9-Carbene-9-Borafluorene Monoanion. *Angew. Chem. Int. Ed.* **2021,** *60*, 13065-13072 ; (i) Budy, H.; Kaese, T.; Bolte, M.; Lerner, H.-W.; Wagner, M., A Chemiluminescent Tetraaryl Diborane(4) Tetraanion. *Angew. Chem. Int. Ed.* **2021,** *60*, 19397-19405 ; (j) Trageser, T.; Bebej, D.; Bolte, M.; Lerner, H.-W.; Wagner, M., B–B vs. B–H Bond Activation in a (μ-Hydrido)diborane(4) Anion upon Cycloaddition with CO2, Isocyanates, or Carbodiimides. *Angew. Chem. Int. Ed.* **2021,** *60*, 13500-13506 ; (k) Wentz, K. E.; Molino, A.; Freeman, L. A.; Dickie, D. A.; Wilson, D. J. D.; Gilliard, R. J., Jr., Systematic Electronic and Structural Studies of 9-Carbene-9-Borafluorene Monoanions and Transformations into Luminescent Boron Spirocycles. *Inorg. Chem.* **2022,** *61*, 17049-17058 ; (l) Wentz, K. E.; Molino, A.; Freeman, L. A.; Dickie, D. A.; Wilson, D. J. D.; Gilliard, R. J., Jr., Activation of Carbon Dioxide by 9-Carbene-9-borafluorene Monoanion: Carbon Monoxide Releasing Transformation of Trioxaborinanone to Luminescent Dioxaborinanone. *J. Am. Chem. Soc.* **2022,** *144*, 16276-16281 ; (m) Barker, J. E.; Obi, A. D.; Dickie, D. A.; Gilliard, R. J., Jr., Boron-Doped Pentacenes: Isolation of Crystalline 5,12- and 5,7-Diboratapentacene Dianions. *J. Am. Chem. Soc.* **2023,** *145*, 2028-2034 ; (n) Sarkar, S. K.; Hollister, K. K.; Molino, A.; Obi, A. D.; Deng, C.-L.; Tra, B. Y. E.; Stewart, B. M.; Dickie, D. A.; Wilson, D. J. D.; Gilliard, R. J., Jr., Bis(9-Boraphenanthrene) and Its Stable Biradical. *J. Am. Chem. Soc.* **2023,** *145*, 21475-21482 ; (o) Wentz, K. E.; Molino, A.; Freeman, L. A.; Dickie, D. A.; Wilson, D. J. D.; Gilliard Jr., R. J., Approaching Dianionic Tetraoxadiborecine Macrocycles: 10-Membered Bora-Crown Ethers Incorporating Borafluorenate Units. *Angew. Chem. Int. Ed.* **2023,** *62*, e202215772 ; (p) Gilmer, J.; Trageser, T.; Čaić, L.; Virovets, A.; Bolte, M.; Lerner, H.-W.; Fantuzzi, F.; Wagner, M., Catalyst-free diboration and silaboration of alkenes and alkynes using bis(9-heterofluorenyl)s. *Chem. Sci.* **2023,** *14*, 4589-4596 ; (q) Gilmer, J.; Bolte, M.; Virovets, A.; Lerner, H.-W.; Fantuzzi, F.; Wagner, M., A Hydride-Substituted Homoleptic Silylborate: How Similar is it to its Diborane(6)-Dianion Isostere? *Chem. Eur. J.* **2023,** *29*, e202203119
20. Groom, C. R.; Bruno, I. J.; Lightfoot, M. P.; Ward, S. C., The Cambridge Structural Database. *Acta Cryst. B* **2016,** *72*, 171-179 (CSD version 5.42, May 2021 update).
21. Ashe, A. J.; Klein, W.; Rousseau, R., Evaluation of the aromaticity of borepin: synthesis and properties of 1-substituted borepins. *Organometallics* **1993,** *12*, 3225-3231
22. Lavallo, V.; Canac, Y.; Präsang, C.; Donnadieu, B.; Bertrand, G., Stable Cyclic (Alkyl)(Amino)Carbenes as Rigid or Flexible, Bulky, Electron-Rich Ligands for Transition-Metal Catalysts: A Quaternary Carbon Atom Makes the Difference. *Angew. Chem. Int. Ed.* **2005,** *44*, 5705-5709
23. Arduengo, A. J.; Krafczyk, R.; Schmutzler, R.; Craig, H. A.; Goerlich, J. R.; Marshall, W. J.; Unverzagt, M., Imidazolylidenes, imidazolinylidenes and imidazolidines. *Tetrahedron* **1999,** *55*, 14523-14534
24. Kuhn, N.; Kratz, T., Synthesis of Imidazol-2-ylidenes by Reduction of Imidazole-2(3H)-thiones. *Synthesis* **1993,** *1993*, 561-562
25. Xu, X.; Takebayashi, S.; Hanayama, H.; Vasylevskyi, S.; Onishi, T.; Ohto, T.; Tada, H.; Narita, A., 6,6′-Biindeno[1,2-b]anthracene: An Open-Shell Biaryl with High Diradical Character. *J. Am. Chem. Soc.* **2023**, 10.1021/jacs.2c13890,
26. Biradicals and Triplet-State Molecules. In *Electron Spin Resonance Spectroscopy of Organic Radicals*, 2003, https://doi.org/10.1002/3527601627.ch11pp 386-404.
27. Yang, W.; Krantz, K. E.; Freeman, L. A.; Dickie, D. A.; Molino, A.; Frenking, G.; Pan, S.; Wilson, D. J. D.; Gilliard, R. J., Jr.,

Persistent Borafluorene Radicals. *Angew. Chem. Int. Ed.* **2020,** *59*, 3850-3854
28. Bleaney, B.; Bowers, K. D., Anomalous paramagnetism of copper acetate. *Proc. Math. Phys. Eng. Sci. P ROY SOC A-MATH PHY* **1952,** *214*, 451-465
29. Soda, T.; Kitagawa, Y.; Onishi, T.; Takano, Y.; Shigeta, Y.; Nagao, H.; Yoshioka, Y.; Yamaguchi, K., Ab initio computations of effective exchange integrals for H–H, H–He–H and Mn2O2 complex: comparison of broken-symmetry approaches. *Chem. Phys. Lett.* **2000,** *319*, 223-230
30. Neese, F., Definition of corresponding orbitals and the diradical character in broken symmetry DFT calculations on spin coupled systems. *J Phys Chem Solids* **2004,** *65*, 781-785
31. Guo, Y.; Sivalingam, K.; Valeev, E. F.; Neese, F., SparseMaps—A systematic infrastructure for reduced-scaling electronic structure methods. III. Linear-scaling multireference domain-based pair natural orbital N-electron valence perturbation theory. *J. Chem. Phys.* **2016,** *144*, 094111
32. Shimoi, M.; Kevlishvili, I.; Watanabe, T.; Maeda, K.; Geib, S. J.; Curran, D. P.; Liu, P.; Taniguchi, T., The Thermal Rearrangement of an NHC-Ligated 3-Benzoborepin to an NHC-Boranorcaradiene. *Angew. Chem. Int. Ed.* **2020,** *59*, 903-909
33. Ashe III, A. J.; Kampf, J. W.; Nakadaira, Y.; Pace, J. M., Aromatic Boron Heterocycles: The Generation of 1 H-Borepin and the Structure of Tricarbonyl(1-phenylborepin)molybdenum. *Angew. Chem. Int. Ed.* **1992,** *31*, 1255-1258
34. Konishi, A.; Kubo, T., Benzenoid Quinodimethanes. *Top. Curr. Chem.* **2017,** *375*, 83

For Table of Contents Only: